

Metal Heptafluoroisopropyl (M-hfip) Complexes for Use as hfip Transfer Agents

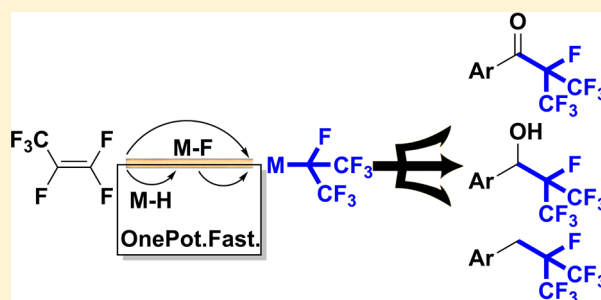
Nicholas O. Andrella,[†] Karen Liu,[†] Bulat Gabidullin,[†] Monica Vasiliu,[‡] David A. Dixon,[‡] and R. Tom Baker^{*,†}

[†]Department of Chemistry and Biomolecular Sciences and Center for Catalysis Research and Innovation, University of Ottawa, Ottawa, Ontario K1N 6N5, Canada

[‡]Department of Chemistry, The University of Alabama, Tuscaloosa, Alabama 35487, United States

Supporting Information

ABSTRACT: New coinage-metal heptafluoroisopropyl (L_nM -hfip) complexes are synthesized from the metal fluoride and inexpensive hexafluoropropene ($M = Ag, Cu$; $L = PPh_3, 2,2,6,6$ -tetramethylpiperidine (Htmp)). Reaction of the silver Htmp complex with a Ni dibromide complex led to efficient hfip transfer to afford $L_2NiBr(hfip)$ ($L = 2$ -ethylpyridine). Treatment of the Ni-hfip complex with $ZnPh_2$ gave the corresponding $L_2NiPh(hfip)$ complexes, which were investigated for reductive elimination of $PhCF(CF_3)_2$. Although the desired reductive elimination proved unsuccessful, addition of carbon monoxide to $L_2NiPh(hfip)$ effected an efficient heptafluoroisopropyl carbonylative cross-coupling. Further, while the silver complex does not undergo hfip transfer to organic electrophiles, the copper complex (phen)(PPh_3) $Cu(hfip)$ (**3b**) effectively transfers the hfip unit to various substrates. We investigated the scope of **3b** with acid chlorides toward the synthesis of perfluoroisopropyl aryl ketones. Additionally, reaction conditions for hfip transfer to *p*-fluorobenzyl bromide and *p*-fluorobenzaldehyde were identified. As a bonus, **3b** was easily generated on a gram scale using commercially available copper hydride by taking advantage of a rapid hydrodefluorination to generate “Cu–F” in situ. Aspects of the observed reactivity are supported by DFT calculations.



INTRODUCTION

Fluorinated carbon fragments, i.e. fluoroalkyls and -aryls, have become quite common in many applications.^{1,2} In the pharmaceutical industry,^{3,4} for example, many household drugs now contain these functional groups,⁵ which offer benefits in metabolic stability, solubility, lipophilicity, and bioavailability. Many of these fluoroalkyl-containing drugs have become “blockbusters”, such as Celebrex, Prevacid, and Pantoprazole.

While many such fragments can be envisioned, only a few are currently readily accessible. For example, trifluoromethylation reactions have seen a period of rapid growth spurred by unique biological applications.⁶ However, installation of other fluoroalkyl fragments such as CF_2H ,⁷ C_2F_5 ,⁸ $OFCF_3$,⁹ and SCF_3 ¹⁰ remains challenging. There has also been a huge investment in identifying new biologically active agents for use in both the agrochemical and pharmaceutical industries. For example, the heptafluoroisopropyl (hfip) group has recently been incorporated into insecticides (Figure 1),¹¹ prompting our current study of its synthesis, coordination chemistry, and transfer to organic electrophiles.

The success and application of fluoroalkylation routes generally hinges on the stability and ease of access of the critical reagent.

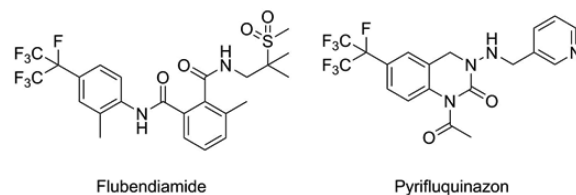


Figure 1. Biologically active compounds containing hfip group.

The Ruppert–Prakash reagent Me_3Si-CF_3 , for example, has seen widespread adoption primarily because of its moderate cost and ready availability.¹² Recently, Grushin et al. successfully prepared a series of $[Cu]CF_2CF_3$ complexes generated from pentafluoroethane,¹³ and Vivic et al. developed a zinc reagent of the type $[Zn]CF_2H$.¹⁴ In both cases, the cost of preparation for these reagents remains low by using base metals and readily available hydrofluoroalkanes. The reactivity of these reagents depends heavily on the choice of ancillary ligand, with 1,10-phenanthroline (phen) giving rise to increased reactivity—such as the (phen) $Cu(CF_3)$ Trifluoromethylator.¹⁵ In this report, we find that changes in the coordination

Received: November 20, 2017

chemistry of copper leads to improved transfer of the hfp fragment to organic electrophiles.

To date, methodologies for the introduction of the hfp group to organic molecules remain scarce. One can generate the hfp nucleophile as the hfp anion $[\text{CF}(\text{CF}_3)_2]^-$ (Figure 2A)¹⁶ or the metal complex $[\text{M}]\text{-hfp}$ (Figure 2B).¹⁷ In these

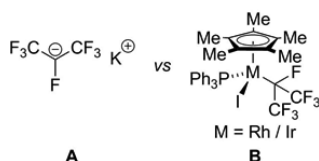
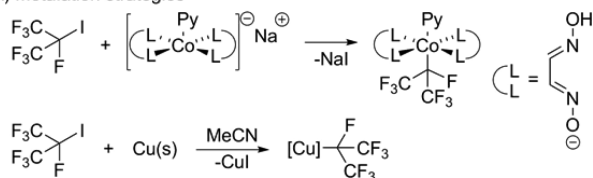


Figure 2. Heptafluoroisopropyl anion vs M-hfp complex.

procedures, two reagents provide a foundation to access the hfp moiety. The more obvious of the two is 2-iodoheptafluoropropane, which has been successfully metalated to yield hfp complexes (Scheme 1A)¹⁸ Alternatively, one can generate

Scheme 1. (A) Metalation of Heptafluoro-2-iodopropane and (B) Addition of M–F to Hexafluoropropene

A) Metalation strategies



B) Insertion strategy



similar compounds from hexafluoropropene (HFP) and a source of fluoride (Scheme 1B).¹⁹ This route benefits from the significantly less expensive starting material (23.7 (HFP) vs 192 \$/mol (Ihfp)), and HFP can be generated selectively from waste polytetrafluoroethylene (PTFE).²⁰

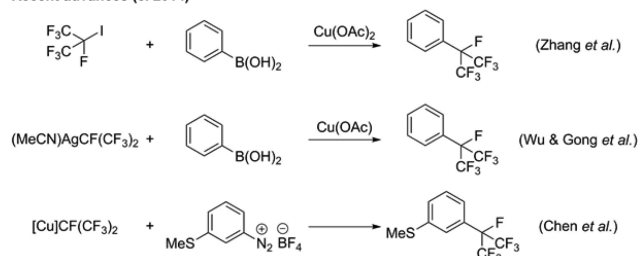
In reports that explore such reactivity, four reagents stand out: the hfp anion and hfp complexes of cadmium, silver, and copper (Scheme 2).²¹ Evidently, each system has its own drawbacks, which could possibly be remediated with the development of new hfp organometallic reagents. Herein, we report the synthesis and characterization of new Cu, Ni, and Ag hfp complexes. The reactivity of each compound is then tested with simple organic electrophiles to determine the nucleophilicity.

RESULTS AND DISCUSSION

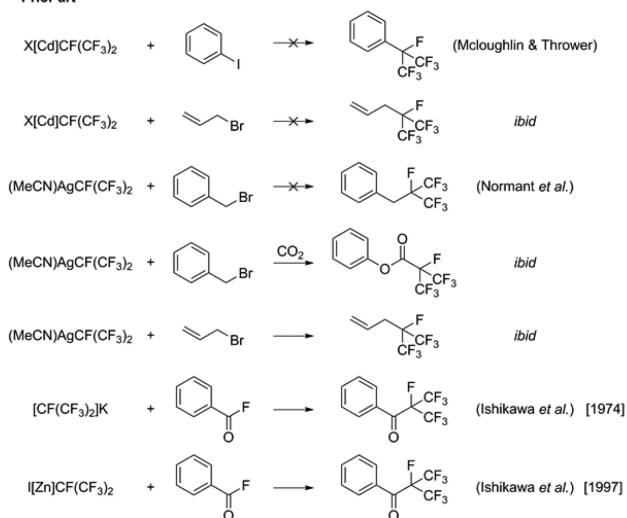
Synthesis and Characterization of a Silver hfp Complex. Following a modified literature procedure,^{19a} the new silver hfp complex **1** was prepared directly from HFP and silver fluoride in the presence of 2,2,6,6-tetramethylpiperidine (Htmp) (Scheme 3). As is typical for such reactions, only a single isomer is observed. The metal fluoride inserts HFP such that the less sterically hindered and the more δ^+ carbon ($=\text{CF}_2$) is oriented toward the fluoride. This choice of ligand was inspired by previous work with AgCF_3 complexes,²² to target the neutral compound (vs $[\text{Ag}(\text{CF}_3)_2]^-$). The colorless powder **1** is slightly unstable at room temperature, becoming

Scheme 2. Reported Reactions of hfp Compounds

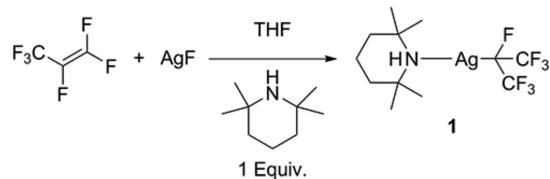
Recent advances (c. 2014)



Prior art



Scheme 3. Synthesis of Compound 1



progressively grayer over time. However, this did not preclude the collection of single-crystal X-ray diffraction data (Figure 3).

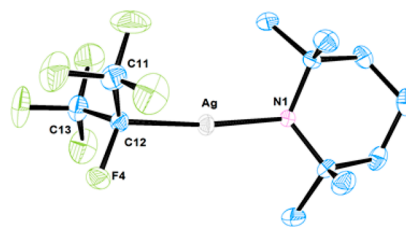


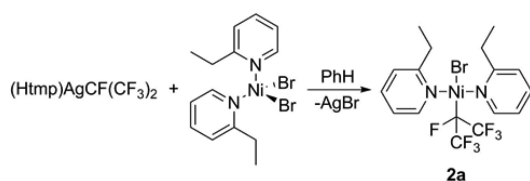
Figure 3. ORTEP representation of the molecular structure of **1**. Thermal ellipsoid probabilities are set to 35%, with hydrogen atoms omitted for clarity.

The molecular structure of complex **1** exhibits a linear coordination about Ag and features a hydrogen bond interaction ($\text{N}\cdots\text{H}\cdots\text{F}$) between the isopropyl fluoride (F4) and the tetramethylpiperidine amine ($\text{N1}\cdots\text{H1}'$) from the neighboring complex in the crystal lattice (see Figure S40 in the Supporting Information). There is a slight distortion from linearity with the shortest $\text{C12}\text{-Ag}\text{-N1}$ angle being 173° .

The ^{19}F NMR spectrum of **1** in C_6D_6 is consistent with the structure determined in the solid state. Whereas the trifluoromethyl group displays a chemical shift difference for the ^{106}Ag and ^{107}Ag isotopomers, the *i*Pr fluoride does not and neither resonance displays Ag–F coupling. Consistent with previous reports, on dissolution in more polar and coordinating solvents an equilibrium between $(\text{Htmp})\text{Ag}[\text{CF}(\text{CF}_3)_2]$ and $\text{Ag}^+[\text{Ag}\{\text{CF}(\text{CF}_3)_2\}_2]^-$ is evident, with the neutral complex being favored.^{17g}

Synthesis and Characterization of Nickel hfp Complexes. With the stable Ag complex **1** in hand, we proceeded to transmetalate the hfp fragment to other transition-metal halides.²³ Generally, the reaction with transition-metal halides led to decomposition of **1** by formation of HFP (β -fluoride elimination) or 2*H*-heptafluoropropane. Reaction with bis(2-ethylpyridine)nickel dibromide in benzene, however, yielded the singly transmetalated product **2a** (Scheme 4). Even when an excess of **1** was used, only **2a** was observed.

Scheme 4. Synthesis of Compound **2a**



The nickel atom of complex **2a** adopts a square-planar geometry with the hfp and bromide trans to each other (Figure 4). While the $\text{C}_\alpha\text{--F}$ bond appears to be significantly longer²⁴

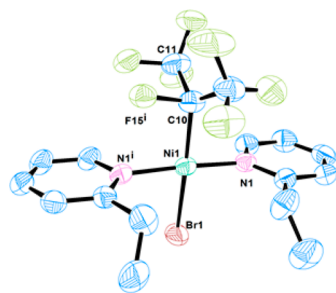


Figure 4. ORTEP representation of the disordered molecular structure of **2a** (ethyl groups can be syn, anti or anti, anti to hfp). Thermal ellipsoid probabilities are set to 35%, with hydrogen atoms omitted for clarity.

than that in **1** (1.59 Å (average) vs 1.420(2) Å in **1**), this is likely an artifact of the disorder in the crystal structure, as the calculated value is in line with other complexes (Table 1).

The ^1H NMR spectrum of **2a** has three broad signals centered at δ 4.5, 5.2, and 9.4, respectively. These are assigned

Table 1. Selected Bond Lengths^a

	1	2a	2c	3a	3b
M–C	2.11/2.14	2.00/2.04	2.00	2.00/2.04	2.00/2.04
$\text{C}_\alpha\text{--F}$	1.42/1.42	1.60 ^c /1.42	1.44	1.43/1.43	1.44/1.43
$\text{C}_\beta\text{--F}^b$	1.32/1.36	1.35/1.36	1.35	1.35/1.37	1.34/1.37

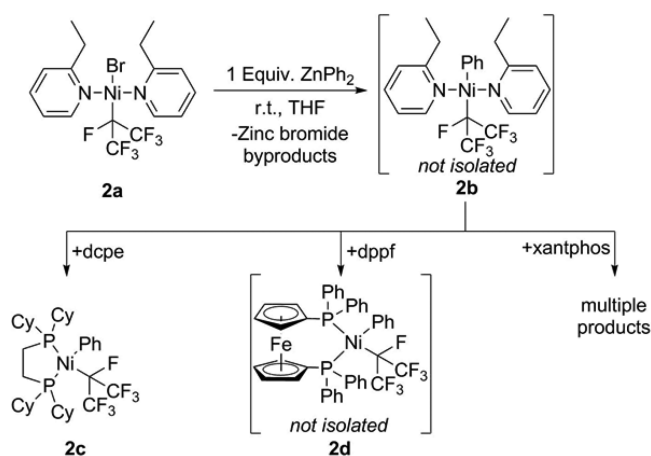
^aAll values are rounded and are given in Å: experimental/calculated.

^bAverage for calculated values at the DFT/B3LYP level. ^cAccuracy likely affected by disorder.

to the CH_2Et and CHpy fragments which reside closest to the metal center. The dynamic process that contributes to these broad resonances is most evident in the variable-temperature ^{19}F NMR spectrum that exhibits the expected doublet and septet resonances only at elevated temperature (Figure S8). At room temperature the inequivalent CF_3 resonances are likely due to hindered rotation about the Ni–C and Ni–N bonds in the two rotamers observed in the solid-state structure.

As **2a** can be considered the oxidative addition product of $\text{BrCF}(\text{CF}_3)_2$ to nickel(0), it may serve as a potential platform to study the cross-coupling synthesis of $\text{ArCF}(\text{CF}_3)_2$. To model such a reaction, we selected diphenylzinc as a potential coupling partner. Immediately upon addition of the zinc reagent to a solution of **2a** in THF, a reaction was observed to form complex **2b** (Scheme 5). This new complex (not isolated) was

Scheme 5. Synthesis of Phenyl Ni-hfp Complexes **2b–d**



then treated in situ with bis(phosphines) to give stable products: 1,2-bis(dicyclohexylphosphino)ethane (dcpe; **2c**), 1,1'-bis(diphenylphosphino)ferrocene (dpfp; **2d** (not isolated)), and xantphos (multiple products).

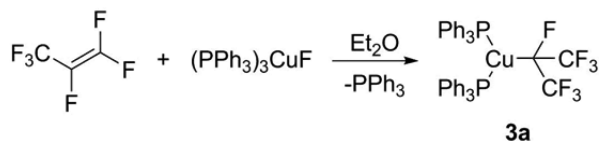
Complex **2c** was isolated as a bright yellow powder and crystallized from acetonitrile. The molecular structure of **2c** shows a distorted-square-planar Ni center with the hfp and the phenyl cis to each other (see Figure S1 in the Supporting Information). The $\text{C}_\alpha\text{--F}$ bond distance (1.437 Å) is now closer in length to that in complex **1**.

Synthesis and Characterization of Copper hfp Complexes. Reaction of **1** with copper chloride in benzene produces the solvated Cu-hfp complex disclosed previously^{17c}

and used extensively in arylboronic acid cross-coupling reactions^{21a} and others.^{18b,21} Looking to avoid the use of the costlier silver fluoride starting material (928 \$/mol), we endeavored to synthesize the Cu complex from commercially available copper fluoride dihydrate (43 \$/mol) and triphenylphosphine (45\$/3 mol). The choice of copper fluorides is limited, since only a few have been reported and/or isolated,²⁵ with $(\text{PPh}_3)_3\text{CuF}$ being successfully used as a source of nucleophilic fluoride. In one example, Szabó et al. demonstrated the substitution of allylic C–X bonds ($\text{X} = \text{Br}, \text{Cl}, \text{OTf}$) using said reagent to synthesize allylic C–F compounds.²⁶ Similarly, Grushin et al. employed this complex to easily generate CuCF_3 from Me_3SiCF_3 .²⁷ In this regard, we expected the coinage-metal fluoride to yield a net addition of Cu–F across the HFP double bond, as seen with AgF.

The copper(I) fluoride complex $\text{CuF}(\text{PPh}_3)_3$ was synthesized as previously reported,^{24a} and treatment with HFP in Et_2O over a 24 h period afforded the hfp complex **3a** in high yield (80%) and excellent purity (>90%, Scheme 6). Solvents of

Scheme 6. Synthesis of **3a** from HFP and Copper(I) Fluoride



higher polarity yielded impurities that are not trivially separated from **3a**. Moreover, the use of dichloromethane or *N,N*-dimethylformamide (DMF) yielded no product and only HFP oligomers. Like the previously reported pentafluoroethyl copper complex,²⁸ the molecular structure of **3a** features a hfp group and two PPh_3 ligands in a trigonal-planar array about the copper (Figure 5 (left)). As expected, the Cu–C bond

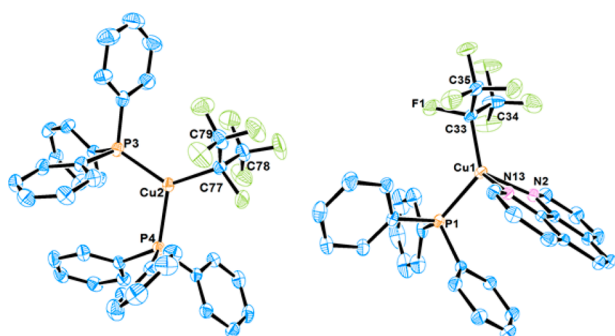
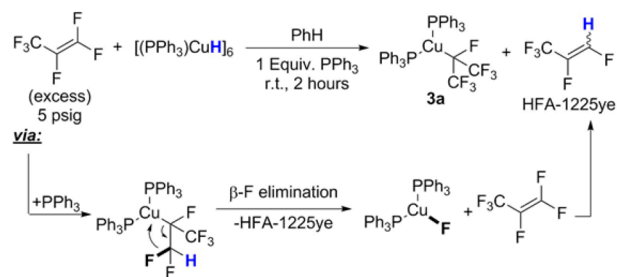


Figure 5. ORTEP representation of the molecular structures of (left) **3a** and (right) **3b**. Thermal ellipsoid probabilities are set to 35%, with hydrogen atoms omitted for clarity.

(2.003(3) Å) is shorter than the Ag–C bond (2.114(2) Å) but is like those in the Cu– CF_2CF_3 (1.99 Å) and Cu– CF_3 (2.025(7) Å) analogues. On this note, the C_α –F bond distance gets progressively smaller with decreasing fluoroalkyl size (1.44 Å for **3a** vs 1.40 and 1.39 Å for CF_2CF_3 and CF_3 , respectively).

As the reaction to form **3a** was slow—likely related to the limited solubility of $[(\text{PPh}_3)_3\text{CuF}]$ in Et_2O —we sought an alternate Cu–X precursor that upon rapid insertion of HFP would undergo β -fluoride elimination to Cu–F followed by subsequent addition of HFP to yield **3a**. For example, Ogoshi et al. have taken advantage of β -fluoride elimination of a copper complex to generate fluorostyrenes.²⁹ To avoid side reactions, we selected X such that the produced fluoroalkene would be a gas at room temperature. We thus turned to commercially available $[(\text{PPh}_3)_3\text{CuH}]_6$ (Stryker's reagent). Although copper hydride has been used for hydrodefluorination of ArF compounds,³⁰ it has never been used with fluoroalkenes. When $[(\text{PPh}_3)_3\text{CuH}]_6$ with an additional 1 equiv of PPh_3 per Cu is exposed to HFP in benzene, it reacts in <2 h to give **3a** in excellent yield (81% based on $[(\text{PPh}_3)_3\text{CuH}]_6$, Scheme 7). Moreover, addition of phen to **3a** in Et_2O gave $[(\text{phen})(\text{PPh}_3)_2\text{Cu}(\text{hfp})]$ (**3b**) in high yield (>80% based on $(\text{PPh}_3)_2\text{Cu}(\text{hfp})$) as a bright orange powder. This change in coordination number and ligand did not have a profound effect

Scheme 7. Synthesis of **3a** from HFP and Stryker's Reagent



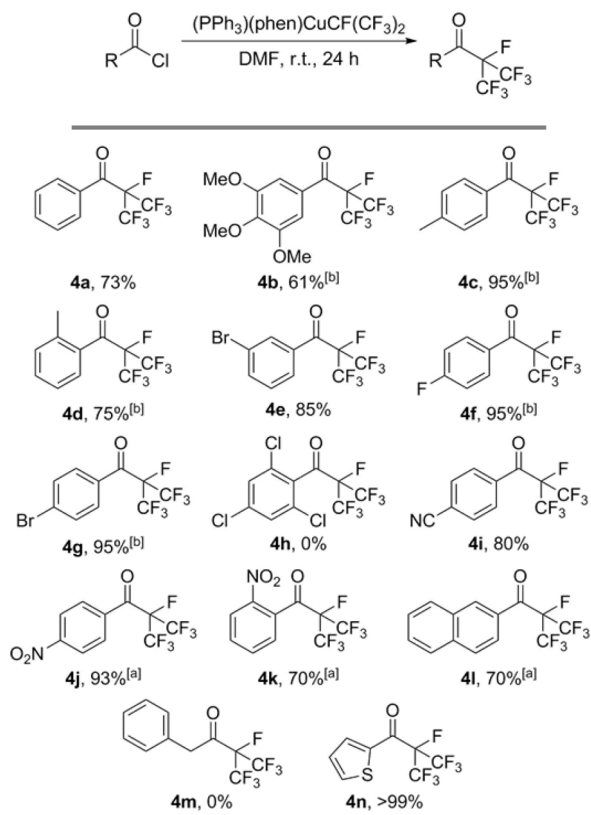
on the Cu–C or C_α –F bond lengths (Figure 5 (right) and Table 1).

The ^{19}F NMR spectrum of **3a** in C_6D_6 shows an unusually broad resonance for C_α –F, indicating some fluxional behavior. This is supported by a broad signal in the ^{31}P NMR spectrum at –5 ppm for both PPh_3 ligands. While **3b** in C_6D_6 reveals a similar trend in the ^{31}P NMR spectrum (broad resonance at –5 ppm), the ^{19}F NMR spectrum now consists of sharp resonances with the typical $^3J_{\text{FF}}$ coupling constant (FC– CF_3) being quite apparent, although no J_{PF} value could be identified. The ^1H NMR spectrum also shows broadening of the signal assigned to phen-H lying closest to the metal center, resulting presumably from fast cleavage and re-formation of the Cu– PPh_3 bond.

Reactivity of M-hfp Complexes with Aroyl Chlorides.

Having these four new M-hfp complexes in hand, we proceeded to test their reactivity with benzoyl chloride to determine which one may be a suitable platform for further nucleophilic studies. First, when **1** was mixed with benzoyl chloride in many solvents, no reaction was observed. This is in line with previously described reactivity for the analogous compound $(\text{MeCN})\text{Ag}[\text{CF}(\text{CF}_3)_2]$.^{17h} Second, when **2a** was mixed with benzoyl chloride, immediate formation of $\text{HCF}(\text{CF}_3)_2$ (Hhfp) was observed. In contrast, when **3a** or **3b** was mixed with benzoyl chloride in DMF, both produced fluorinated ketone **4a** in moderate (50%) and high (75%) yields, respectively. In the case of **3a** the reagent is unstable under the reaction conditions and produces an equivalent amount of benzoyl fluoride, arising presumably from β -fluoride elimination with concomitant formation of HFP. Optimizing the reaction of **3b** with benzoyl chloride, we found that DMF was required; all other solvents tested yielded no product and gave exclusively Hhfp. The reaction proceeds readily at room temperature over 24 h.

Existing methods for the synthesis of these compounds have been limited either by (a) generation of the $[\text{CF}(\text{CF}_3)_2]^-$ anion and accompanying HFP oligomers^{16a} or (b) the use of acid fluorides, generated from acid chlorides.^{17i,31} The reaction can be applied to a wide range of acid chlorides bearing various functional groups, including halide (**4e–g**), CN (**4i**), ether (**4k**), alkyl (**4c**), nitro (**4j,k**), naphthyl (**4l**), and thiophene (**4n**; Scheme 8). Some steric effects could be observed. For example, the ortho derivatives gave lower yields (**4d,k**). The extent of this effect is better measured using the 2,4,6-chloro-substituted benzoyl chloride that does not react with **3b**. In general, the electron-rich aroyl chlorides always gave lower yields, presumably due to reversibility under the reaction conditions. This is more evident in the case of 3,4,5-trimethoxybenzoyl chloride, for which the yield drops off as the reaction progresses. Similarly, this highlights the inherent difficulty in isolating these products, as the hfp group is readily substituted and therefore demands rigorously dry conditions. To

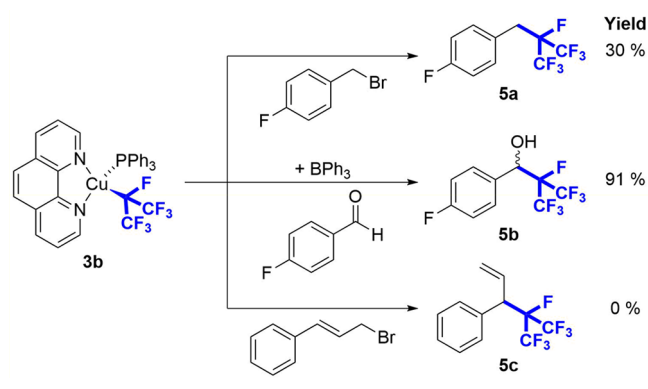
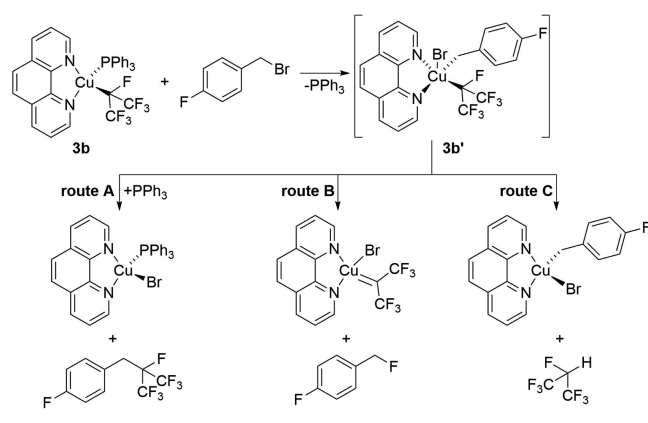
Scheme 8. Perfluoroisopropylation of Aroyl Chlorides^c

^a1 equiv of **3b**. ^b4 h at room temperature. ^cReaction conditions unless specified otherwise: 0.074 mmol of Cu, 0.049 mmol of acid chloride, and 0.027 mmol of internal standard in 0.5 mL of DMF at room temperature for 24 h. The reactions were performed in an NMR tube sealed with a plastic cap and wrapped with Parafilm without stirring. The yields were determined by ¹⁹F NMR spectroscopy with hexafluorobenzene as an internal standard vs moles of electrophile. For details see the Supporting Information.

compound this issue, all of the products are volatile and could not be easily separated from DMF. However, they can be collected as the distillate with DMF.³² Noticeably, phenyl acetyl chloride, the only alkyl acid chloride, does not react with **3b**.

Reactivity of Cu-hfip Complexes with Other Electrophiles. Reactions of **3b** with several other electrophiles generally required ~1.5 equiv of **3b** due to competing formation of Hhfip.³³ Reaction of **3b** with 4-fluorobenzyl bromide (Scheme 9, top) gave an unusually low yield and produced several unidentifiable products on heating to 50 °C. To compound the issue, the product **5a** was unstable under regular workup conditions. In one attempt at isolation of **5a** by column chromatography, no product was collected. Although we expected the formation of benzyl fluoride to arise from β -fluoride transfer, we did not observe concomitant formation of HFP under the reaction conditions.

We suspect that the benzyl fluoride arises from α -fluoride transfer (Scheme 10, route B) from an intermediate copper(III) complex (**3b'**) and is in competition with product formation, corroborating the 30% yield. On the trend of alkyl halides, we found that those vicinal to a ketone do not react with **3a** (e.g., bromoacetophenone). We also found that bulkier benzhydryl halides do not substitute readily. Unfortunately, **5c** was not stable under the reaction conditions and slowly decomposed, precluding its isolation. Finally, aldehydes could be substituted

Scheme 9. Reactions of **3b** with Other ElectrophilesScheme 10. Reaction of **3b** with a Benzyl Bromide and Suspected Decomposition Pathways of **3b'**

by employing a weak Lewis acid as an additive. While **3b** does not react readily with 4-fluorobenzaldehyde, addition of a strong Lewis acid also does not produce the desired product. **3b** itself reacts with both trimethylsilyl trifluoromethanesulfonate (TMSOTf) and trifluoroborane etherate ($\text{BF}_3 \cdot \text{Et}_2\text{O}$). However, addition of triphenylborane gave the desired product **5b** in 91% yield.

Reactivity of Ni(Ph)hfip (2b) toward Reductive Elimination. Upon heating complexes **2b–d** to 66 °C, (a) no reaction (**2c**), (b) decomposition to Hhfip (**2b**), or (c) a mixture of unknown products (**2d**) was observed. With the stable complex **2c** in hand, we attempted to effect the associatively induced reductive elimination by addition of excess triethyl phosphite, 2,6-dimethylphenyl isocyanide, or CO gas. Although addition of triethyl phosphite had no effect, the isocyanide reacted immediately to give a mixture of unidentified products. Addition of CO (3 atm) to **2c** (in either THF or benzene-*d*₆) at 50 °C instead produced the ketone in 90% yield (Scheme 11), with some Hhfip produced in a side reaction.

Scheme 11. Carbonylation and Reductive Elimination of the hfip Group

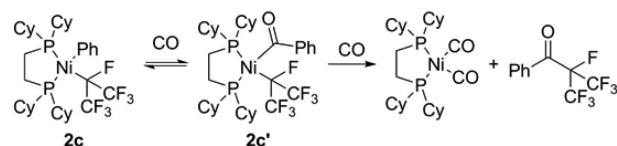
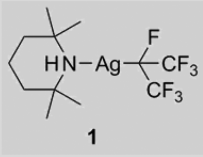

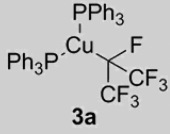
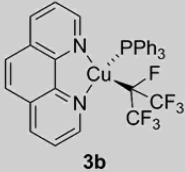


Table 2. Bond Dissociation Energies (BDE, ΔH_{0K} , and ΔG_{298K} at the B3LYP/DZVP2/aug-cc-pvdz-pp(M) Level in kcal/mol) and Charge Distribution of Some Reported Complexes

Complex				
Homolytic BDE $\Delta H_{0K} / \Delta G_{298K}$ $\Delta G_{298K}(\text{DMF})$	71.1/57.3/62.9	46.4/28.4/22.2	80.7/64.1/66.6	55.1/40.0/44.1
Heterolytic BDE $\Delta H_{0K} / \Delta G_{298K} /$ $\Delta G_{298K}(\text{DMF})$	133.9/122.1/33.8	116.4/98.0/12.6 ^a	90.3/74.3/1.8	86.4/72.6/32.4
Charge (NBO NPA)	M(0.555), C- ⁱ Pr ^F (-0.186)	M(0.716), C- ⁱ Pr ^F (-0.097)	M(0.598), C- ⁱ Pr ^F (-0.275)	M(0.748), C- ⁱ Pr ^F (-0.260)

^aThe Ni cation has a triplet ground state.

This suggests that catalytic perfluoroalkylcarbonylation³⁴ using nickel could be possible and will be explored further in due course.

Computational Chemistry. To provide insight into these reactivity trends, we carried out DFT calculations (at the B3LYP/DZVP2/aug-cc-pvdz-pp(M) level; Table 2). The calculated bond distances are in good agreement with experiment (Table 1). The calculated ³¹P gas-phase NMR chemical shifts are within about 12 ppm of experiment, while those for ¹⁹F differ by ~20–30 ppm for CF₃ⁱPr^F and the CFⁱPr^F (see the Supporting Information). This is typical of the usual errors in calculated chemical shifts for these nuclei.

There are two types of bond dissociation energies (BDEs) to consider for this system: homolytic with formation of a metal-centered radical and the perfluoroisopropyl radical and heterolytic with formation of a metal-centered cation and the perfluoroisopropyl anion. In the gas phase, homolytic cleavage always requires less energy than heterolytic cleavage. However, in solution, heterolytic cleavage can become favored due to solvation of the ions. In the gas phase, **1** and **3a** have significantly higher homolytic BDEs than do **2a** and **3b**, with **2a** having the lowest homolytic BDE. In DMF solution **3a** is predicted to have a heterolytic BDE of close to 0 kcal/mol and **2a** is predicted to have a heterolytic BDE of just above 10 kcal/mol. In contrast, **1** and **3b** have heterolytic BDEs of slightly greater than 30 kcal/mol in solution. The difference between the heterolytic BDEs in **3a** and **3b** arises from the bulky cation generated from **3b**, which is not as well solvated as is the smaller cation generated from **3a**. Furthermore, the perfluoroisopropyl anion can release fluoride to generate CF₃(F)C=CF₂. The fluoride affinity of perfluoropropene is $\Delta H_{298K} = 46.3$ kcal/mol and $\Delta G_{298K} = 37.2$ kcal/mol in the gas phase at the G3MP2 level³⁵ (see the Supporting Information). Inclusion of a solvent effect leads to the result that it is exothermic to release F⁻ from the ⁱPr^F anion by -6.3 kcal/mol.

The lack of reactivity observed for **1** is consistent with the calculated BDEs. The instability of **3a** is also consistent with the low energy for heterolytic cleavage and should be very sensitive to reaction conditions, especially as F⁻ can be generated from

the perfluoroisopropyl anion. The BDEs for **2a** suggest that both heterolytic and homolytic cleavage could occur.

CONCLUSIONS

In summary, we have prepared a series of stable M-hfip complexes and investigated their reactivity. Isolation of the first stable Ni-hfip complexes demonstrates their potential for new cross-coupling reactions. The synthesis of **2a** was enabled by the underexploited salt metathesis reaction between Ag-R^F and transition-metal halides, whereby previous attempts had yielded ionic species such as [Rh]⁺[Ag(R^F)₂]⁻,^{17f} the prior paradigm being that only copper complexes could be synthesized.^{17b,21a} Further, this may enable access to metals in low oxidation states without the need for reduction. However, as demonstrated herein, a judicious choice of transition-metal starting material and ligand is necessary for success of these transfers.

Although the aforementioned reaction does yield the copper complex, we have discovered a new convenient synthesis of Cu-hfip complexes **3a,b**. An easily prepared, air-stable copper fluoride can be used to synthesize new Cu-hfip complexes, thus bypassing the need for silver. We have optimized these conditions to prevent side reactions, such as HFP oligomerization, which we found can occur in media other than Et₂O. Still, we wished to improve the reaction efficiency by decreasing the reaction time (likely limited by poor solubility of the Cu-F complex) and increasing the atom efficiency (Cu-F synthesis <50%). We have thus shown that a commercially available copper hydride can readily hydrodefluorinate HFP, generating Cu-F in situ which reacts rapidly with HFP to give the Cu-hfip complex.

On evaluating the reactivity of all new M-hfip complexes toward electrophiles, we showed that Cu complexes **3a,b** readily transfer the hfip fragment to benzoyl chloride. These findings have been supported by DFT calculations, which yielded parameters against which to compare for suspected reactivity/stability trends. It may serve as a preliminary screening mechanism to identify successful candidates to further expand the scope of hfip transfers.

The trend in BDE explains quite readily the propensity for the formation of Hhfp or HFP over the course of the reaction. This is especially true in the case of **3b**, where without judicious choice of solvent (e.g., DMF) the desired reaction does not occur, although a balance must be struck between the M–C BDE (**3b** \ll **3a**) and the desired reactivity. As a bonus **3b** also possesses a greater positive charge at Cu that could be beneficial for reactivity with less activated substrates.

Ongoing work is focused on (a) expanding the range of electrophiles that can undergo substitution with **3b** and (b) exploring conditions for *catalytic* cross-coupling for both **2c** and **3b** or analogues thereof. Preliminary results of the stoichiometric substitution reactions with **3b** are encouraging and indicate an enhanced reactivity of said reagent. Full details of these results will be published in due course.

EXPERIMENTAL SECTION

General Procedures. Experiments were conducted under nitrogen, using Schlenk techniques or an MBraun glovebox. All solvents were deoxygenated by purging with nitrogen. Hexanes, diethyl ether (Et₂O), 1,2-dimethoxyethane (DME), and tetrahydrofuran (THF) were dried on columns of activated alumina using a J. C. Meyer (formerly Glass Contour) solvent purification system. Benzene-*d*₆ (C₆D₆) was dried by stirring over activated alumina (ca. 10 wt %) overnight, followed by filtration. All solvents were stored over activated (heated at ca. 250 °C for >10 h under vacuum) 4 Å molecular sieves, and glassware was oven-dried at 120 °C for >2 h. The following chemicals were obtained commercially, as indicated: silver fluoride (AgF, Alfa, 99%), hexafluoropropene (HFP, Synquest, 99%), triphenylphosphine (PPh₃, Oakwood Chemical, 99%), copper(II) fluoride dihydrate (CuF₂·2H₂O, Alfa), diphenylzinc (ZnPh₂, Strem Chemicals, 99%), all acid chlorides (Sigma-Aldrich, 99%), 4-fluorobenzyl bromide (Oakwood Chemicals, 99%), 4-fluorobenzaldehyde (Oakwood Chemicals, 99%), 3-bromo-1-phenyl-1-propene (cinnamyl bromide, Sigma-Aldrich, 97%), 2,2,6,6-tetramethylpiperidine (Htmp, Sigma-Aldrich, 99%), 1,10-phenanthroline, anhydrous (phen, Alfa, 99%), 4,5-bis(diphenylphosphino)-9,9-dimethylxanthene (xantphos, Accela, 97%), 1,1'-bis(diphenylphosphino)ferrocene (dppf, Accela, 95%), 1,2-bis(dicyclohexylphosphino)ethane (dcpe, Strem, 98%), triethyl phosphite (P(OEt)₃, Sigma-Aldrich, 99%), and 2,6-dimethylphenyl isocyanide (XylCN, Sigma-Aldrich, 96%). ¹H, ¹⁹F, ³¹P{¹H}, and ¹³C{¹H} NMR spectra were recorded on a 300 MHz Bruker Avance instrument at room temperature (21–23 °C) unless stated otherwise. ¹H NMR spectra were referenced to residual proton peaks associated with the deuterated solvents (C₆D₆: 7.16 ppm). ¹⁹F NMR spectra were referenced to internal standard hexafluorobenzene (C₆F₆, Oakwood, 99%), unless stated otherwise, set to –164.5 ppm. ¹³C{¹H} NMR data were referenced to carbon peaks associated with the solvent (C₆D₆, 128.39 ppm; THF, 67.57 ppm). ³¹P{¹H} NMR data were referenced to external H₃PO₄ (85% aqueous solution), set to 0.0 ppm. Electrospray ionization mass spectral data were collected using an Applied Biosystem API2000 triple quadrupole mass spectrometer. UV–vis spectra were recorded on a Cary 100 instrument, using sealable quartz cuvettes (1.0 cm path length). IR data were obtained on a Nicolet Nexus 6700 FT-IR spectrometer. For **3a**, the sample was prepared by allowing a benzene solution of **1** to evaporate on a NaCl plate under a stream of nitrogen. Elemental analyses were performed by Laboratoire d'analyse élémentaire, Université de Montréal (Montreal, Quebec, Canada). Note that the NMR spectra (¹H, ¹⁹F, ¹⁹F{¹H}, ³¹P{¹H} and ¹³C{¹H}) for the title compounds are displayed in the Supporting Information.

Synthesis of [(Htmp)Ag(hfip)] (1). AgF (500 mg, 3.94 mmol) was placed in a 100 mL ampule and mixed with 15 mL of THF. Colorless Htmp (612 mg, 4.34 mmol) was then added to the slurry. The reaction vessel was attached via a three-way valve to an HFP canister with a regulator and a Schlenk line. The solution was degassed using a regular freeze/pump/thaw method. The HFP was added to the degassed solution with the regulator set to 5 psi. The reaction mixture

was stirred at 25 °C for ~24 h and wrapped in tin foil. The solid became dark green after a few hours. As the reaction progressed, the solution became progressively clear with a slight silver mirror forming. The solution was filtered through a Celite pad (15 mL medium pore fritted funnel), and the remaining solvent was removed in vacuo to yield a colorless powder. A 10 mL portion of hexanes was added, and the solid was collected (30 mL medium pore fritted funnel), washed with hexanes (4 °C, 3 × 5 mL), and dried in vacuo to yield 1.44 g of **1** (3.55 mmol, 90% based on AgF). The isolated material was stored in a refrigerator under nitrogen in an amber container. ¹H NMR (300 MHz, C₆D₆): δ 1.17 (br, 2H, CH₂), 1.06 (m, *J*_{HH} = 6 Hz, 4H, CH₂), 0.76 (br, 12H, Me). ¹⁹F NMR (282 MHz, C₆D₆): δ –68.45 (d, ³*J*_{FF} = 13 Hz, 6F, CF₃), –68.50 (d, ³*J*_{FF} = 13 Hz, 6F, CF₃), –211.03 (d “hept”, ³*J*_{FF} = 13 Hz, ²*J*_{AgF} = 2 Hz, 1F, CFⁱPr^F), –211.12 (d “hept”, ³*J*_{FF} = 13 Hz, ²*J*_{AgF} = 2 Hz, 1F, CFⁱPr^F). ¹³C{¹H} NMR (75 MHz, C₆D₆): δ 17.3 (Htmp), 32.0 (br, Htmp), 37.3 (Htmp), 54.0 (Htmp), 104.1 (“multiplet”, CFⁱPr^F), 127.1 (qdqd, ¹*J*_{CF} = 273 Hz, ²*J*_{CF} = 24 Hz, ³*J*_{CF} = ²*J*_{AgC} = 5 Hz). IR: 3262(w), 2948(w, br), 1452(m, br), 1394(s), 1351(s), 1098(w), 932(s), 734(s), 692(s) cm^{–1}. ESI-MS: *m/z* (%) 562.15 (100), 563.16 (20), 564.15 (95), 566.15 (15) [*M*⁺ – H + 2THF], 142.16 [*L*⁺ – H]. See Figures S2–S4 for ¹H, ¹⁹F, and ¹³C{¹H} NMR spectra.

Synthesis of [(PyEt)₂NiBr(hfip)] (2a). The purple complex [(PyEt)₂NiBr₂]⁵⁹ (1.000 g, 2.31 mmol) was placed in a 100 mL round-bottom flask and mixed with 30 mL of benzene. A 10 mL colorless solution of **1** in benzene (990 mg, 2.37 mmol) was then added to the slurry. The reaction mixture was stirred at 25 °C for 24 h. The solution became progressively pink as the reaction progressed. The deep pink solution with a light yellow precipitate (AgBr) was filtered through a Celite pad (15 mL medium-pore fritted funnel), and the remaining solvent was removed in vacuo to yield a light pink powder. Roughly 5 mL of hexanes was added, and the solid was collected (30 mL medium-pore fritted funnel), washed with hexanes (4 °C, 3 × 5 mL), and dried in vacuo to yield 1.05 g of **2a** (2.00 mmol, 87% based on [(PyEt)₂NiBr₂]). The isolated material was stored at room temperature under nitrogen. UV–vis (1.0 mM in THF): λ_{max} (ε) 495 nm (407 M^{–1} cm^{–1}). ¹H NMR (300 MHz, C₆D₆): δ 1.38 (t, ³*J*_{HH} = 7 Hz, 6H, MeEt), 4.56 (br, 2H, CH₂Et), 5.19 (br, 2H, CH₂Et), 6.23 (td, ³*J*_{HH} = 7 Hz, ⁴*J*_{HH} = 1 Hz, 2H, CHPy), 6.36 (d, ³*J*_{HH} = 7 Hz, 2H, CHPy), 6.54 (td, ³*J*_{HH} = 7 Hz, ⁴*J*_{HH} = 1 Hz, 2H, CHPy), 9.37 (br, 2H, CHPy). ¹⁹F NMR (282 MHz, C₆D₆): δ –68.24 (br, CFⁱPr^F), –68.68 (br, CF₃ⁱPr^F), –70.11 (br, CF₃ⁱPr^F), –204.65 (br, CFⁱPr^F). ¹H NMR (300 MHz, C₆D₆, 50 °C): δ 1.45 (td, ³*J*_{HH} = 7 Hz, ⁴*J*_{HH} = 2 Hz, 6H, MeEt), 4.87 (br, 4H, CH₂Et), 6.34 (t “multiplet”, ³*J*_{HH} = 7 Hz, 2H, CHPy), 6.50 (d, ³*J*_{HH} = 7 Hz, 2H, CHPy), 6.67 (t “multiplet”, ³*J*_{HH} = 7 Hz, 2H, CHPy), 9.49 (br, 2H, CHPy). ¹⁹F NMR (282 MHz, C₆D₆, 50 °C): δ –68.56 (br, CF₃ⁱPr^F), –206.10 (br, CFⁱPr^F). Anal. Calcd for C₁₇H₁₈BrF₇N₂Ni: C, 39.12, H, 3.48, N, 5.37. Found: C, 38.37, H, 3.71, N, 5.16. See Figures S5 and S6 for ¹H and ¹⁹F NMR spectra. See Figures S7 and S8 for ¹H and ¹⁹F NMR spectra at 50 °C.

In Situ Synthesis of [(PyEt)₂Ni(Ph)(hfip)] (2b). The pink complex [(PyEt)₂NiBr(hfip)] (20 mg, 0.04 mmol) was placed in a 5 mL round-bottom flask and mixed with 1 mL of THF. A 1 mL colorless solution of Ph₂Zn in THF (9 mg, 0.04 mmol) was then added to the solution, affording a yellow-brown solution after 10 min that was used as is. ¹⁹F NMR (282 MHz, C₆D₆): δ –66.70 (br, CF₃ⁱPr^F (**2b'**)), –67.39 (“quint”, ³*J*_{FF} = ⁴*J*_{FF} = 9 Hz, CF₃ⁱPr^F (**2b''**)), –68.00 (d, ³*J*_{FF} = 10 Hz, CF₃ⁱPr^F (**2b'''**)), –68.01 (br, CFⁱPr^F (**2b'**)), –69.14 (“quint”, ³*J*_{FF} = ⁴*J*_{FF} = 9 Hz, CF₃ⁱPr^F (**2b'''**)), –197.33 (br, CFⁱPr^F (**2b'**)), –214.80 (sept, ³*J*_{FF} = 9 Hz, CFⁱPr^F (**2b''**)), –215.26 (sept, ³*J*_{FF} = 10 Hz, CFⁱPr^F (**2b'''**)). See Figure S9 for ¹⁹F NMR spectra.

Synthesis of [(dcpe)Ni(Ph)(hfip)] (2c). To a 5 mL solution of complex **2b** in THF (100 mg, 0.19 mmol, vide supra) was added solid dcpe (89 mg, 0.21 mmol). On stirring at 25 °C over 1 h, the solution became progressively lighter yellow with concomitant formation of a black precipitate. The light yellow solution was filtered through a Celite pad (15 mL medium-pore fritted funnel), and the remaining solvent was removed in vacuo to yield a light yellow powder. Roughly 5 mL of acetonitrile was added and the solid was collected (15 mL

medium-pore fritted funnel), washed with Et₂O (4 °C, 3 × 3 mL), and dried in vacuo to yield 105 mg of **2c** (0.14 mmol, 75% based on (PyEt)₂NiBr₂). UV-vis (1.5 mM in THF): λ_{max} (ε) 373 (882), 307 nm (2348 M⁻¹ cm⁻¹). ¹H NMR (300 MHz, C₆D₆): δ 7.89 (m, 2H, Ar), 7.05 (m, 2H, Ar), 6.91 (m, 1H, Ar), 2.5–0.5 (overlap, 48H, Cy and CH₂Et). ¹⁹F NMR (282 MHz, THF): δ -65.19 (dd, ⁴J_{FF} = 5 Hz, ³J_{FF} = 13 Hz, CF₃ⁱPr^F), -169.28 (dsept, ⁴J_{FP} = 96 Hz, ⁴J_{FF} = 13 Hz, CF^FPr^F). ¹³C{¹H} NMR (75 MHz, THF): δ 153.1 (dd, ²J_{PC} = 76 Hz, ²J_{PC} = 43 Hz, CαAr), 137.9 (CAR), 124.9 (CAR), 121.1 (CAR), 36.2 (“multiplet”, dcpe), 34.5 (“multiplet”, dcpe), 29.9–24 (overlap(THF), dcpe), 20.0 (“multiplet”, dcpe). ³¹P{¹H} NMR (121 MHz, THF): δ 57.81 (dd, ³J_{PF} = 96 Hz, ²J_{PP} = 31 Hz, P-*trans*-hfp), 47.75 (dsept, ²J_{PP} = 31 Hz, ⁴J_{PF} = 6 Hz, P-*cis*-hfp). Compound **2c** proved to be quite hygroscopic and sensitive to air and moisture. Collection of elemental analysis data returned a value closest to [(C₇H₅PCH₂CH₂P(O)C₇H₅)-Ni(Ph)(hfp)]·2H₂O]. Anal. Calcd for C₃₅H₅₇F₇NiO₃P₂: C, 53.93; H, 7.37. Found: C, 53.98; H, 7.28. See Figures S10–S13 for ¹H, ¹⁹F, ¹³C{¹H}, and ³¹P{¹H} NMR spectra.

In Situ Synthesis of [(dcpe)Ni(CO)Ph(hfp)] (2c’). A J. Young NMR tube containing a 0.6 mL solution of complex **2c** in C₆D₆ or THF (20 mg, 0.028 mmol) was degassed, and CO (1 atm) was added. The tube was heated for 2 h at 50 °C to produce a mixture [6:7:1] of **2c**, **2c’** and **4a** respectively. ¹⁹F NMR (282 MHz, C₆D₆): δ -66.24 (“quint”, ³J_{FF} = ⁴J_{FF} = 9 Hz, CF₃ⁱPr^F), -67.22 (“quint”, ³J_{FF} = ⁴J_{FF} = 9 Hz, CF₃ⁱPr^F), -167.619 (m, ³J_{FF} = ⁴J_{FF} = 9 Hz, ³J_{FP} = 26 Hz, ³J_{FF} = 120 Hz, CF^FPr^F). ³¹P{¹H} NMR (121 MHz, C₆D₆): δ 45.15 (m, ³J_{FP} = 120 Hz), 39.48 (m, ³J_{FP} = 26 Hz). N.B.: for the reaction to go to completion (yield 90%) 3 atm of CO should be employed. See Figures S21–S24 for ¹⁹F and ³¹P{¹H} NMR spectra of the reaction carried out at 1 atm (30% yield).

In Situ Synthesis of [(dppf)Ni(Ph)(hfp)] (2d). In a J. Young NMR tube containing a 0.6 mL solution of complex **2b** in THF (20 mg, 0.04 mmol) was placed solid dppf (21 mg, 0.04 mmol). The solution became deep orange and was used as is. ¹⁹F NMR (282 MHz, C₆D₆): δ -65.16 (d, ³J_{FF} = 9 Hz, CF₃ⁱPr^F (2d)), -66.30 (“quint”, ³J_{FF} = ⁴J_{FF} = 9 Hz, CF₃ⁱPr^F (2d’)), -67.96 (“quint”, ³J_{FF} = ⁴J_{FF} = 9 Hz, CF₃ⁱPr^F (2d’)), -166.99 (br m, ³J_{FF} = ⁴J_{FF} = 9 Hz, ³J_{FP} = 150 Hz, CF^FPr^F (2d)), -200.42 (sext, ³J_{FF} = ³J_{FF} = ⁴J_{FF} = 9 Hz, CF^FPr^F (2d’)). See Figure S14 for ¹⁹F NMR spectrum.

Synthesis of [(PPh₃)₂Cu(hfp)] (3a). *Method A.* The colorless complex [(PPh₃)₂CuF] (500 mg, 0.56 mmol) was placed in a 100 mL ampule and mixed with 30 mL of Et₂O. The reaction vessel was attached via a three-way valve to an HFP canister with a regulator and a Schlenk line. The solution was degassed using a regular freeze/pump/thaw method. The HFP was added to the degassed solution with the regulator set to 5 psi. The reaction mixture was stirred at 25 °C for ~24 h. A colorless precipitate remained over the course of the reaction. The solvent was removed in vacuo, 10 mL of DME was added, and this solution was filtered through a Celite pad (15 mL medium-pore fritted funnel) to remove unreacted Cu–F. The volatiles were removed in vacuo, and roughly 10 mL of hexanes was added. The solid was collected (15 mL medium-pore fritted funnel), triturated with hexanes (3 × 10 mL), and dried in vacuo to yield 391 mg of **3a** (0.52 mmol, 90% based on (PPh₃)₂CuF). The isolated material was stored at room temperature under nitrogen.

Method B. The red complex [(PPh₃)₂CuH]₆ (5.23 g, 16 mmol based on monomeric unit) and PPh₃ (5.03 g, 19.2 mmol) were placed in a 1 L Schlenk round-bottom flask and mixed with 100 mL of benzene. The reaction vessel was attached via a three-way valve to an HFP canister with a regulator and a Schlenk line. The solution was degassed using a regular freeze/pump/thaw method. The HFP was added to the degassed solution with the regulator set to 5 psi and the reaction mixture stirred at 25 °C for ~2 h. The solution became light yellow. The solvent was removed in vacuo, leaving a buff powder. The powder was dissolved in DME (100 mL) and stirred vigorously. The solution was then filtered (15 mL medium pore fritted funnel) and the solvent removed in vacuo. The solid was collected (30 mL medium-pore fritted funnel), triturated with cold Et₂O (-35 °C, 3 × 20 mL), and dried in vacuo to yield 9.81 g of **3a** (12.96 mmol, 81% based on

((PPh₃)₂CuH)₆). IR: 3053(m,br), 1480(m), 1434(s,sh), 1292(w), 1231(w), 1146(w), 1116(w), 1094(w), 741(s,sh), 639(s,sh) cm⁻¹. ¹H NMR (300 MHz, C₆D₆): δ 6.88 (m, 18H, Ar), 7.31 (m, 12H, Ar). ¹⁹F NMR (282 MHz, C₆D₆): δ -68.93 (br, CF₃ⁱPr^F), -207.98 (br, CF^FPr^F). ³¹P{¹H} NMR (121 MHz, C₆D₆): δ -4.66 (s, PPh₃). Anal. Calcd for C₃₉H₃₀CuF₂P₂: C, 61.87, H, 3.99. Found: C, 63.47, H, 4.12. See Figures S15–S17 for ¹H, ¹⁹F, and ³¹P{¹H} NMR spectra.

Synthesis of (PPh₃)₂(phen)Cu(hfp) (3b). The colorless complex [(PPh₃)₂Cu(hfp)] (500 mg, 0.66 mmol) was placed in a 20 mL scintillation vial and mixed with 10 mL of Et₂O. Phen (130 mg, 0.73 mmol) was then added slowly while the solution was vigorously stirred. The reaction mixture was stirred for 1 h as it changed from clear to deep orange with a significant amount of orange precipitate. Roughly 10 mL of hexanes was added, and the solid was collected (15 mL medium-pore fritted funnel). The solid was dissolved in 10 mL of DME, the solution was filtered through a Celite-padded frit (15 mL medium-pore fritted funnel), 50 mL of hexanes was added, and the solid was collected, washed with hexanes (3 × 10 mL), and dried in vacuo to yield 356 mg of **3b** (0.53 mmol, 80% based on **3a**). The isolated material was stored at room temperature under nitrogen. A second crop of product could be collected by crystallizing from the remaining solution at -35 °C. UV-vis (1.0 mM in benzene): λ_{max} (ε) 395 nm (1276 M⁻¹ cm⁻¹). ¹H NMR (300 MHz, C₆D₆): δ 8.88 (br, 2H, phen), 7.49 (m, 6H, PPh₃), 7.28 (m, 2H, phen), 6.99 (s, 2H, phen), 6.90 (m, 9H, PPh₃), 6.72 (m, 2H, phen). ¹⁹F NMR (282 MHz, C₆D₆): δ -67.39 (d, ³J_{FF} = 10 Hz, CF₃ⁱPr^F), -209.05 (sept, ³J_{FF} = 10 Hz, CF^FPr^F). ³¹P{¹H} NMR (121 MHz, C₆D₆): δ -4.95 (br, PPh₃). Anal. Calcd for C₃₃H₂₃CuF₇N₂P₂: C, 58.71, H, 3.43, N, 4.15. Found: C, 58.18, H, 3.51, N, 4.15. See Figures S18–S20 for ¹H, ¹⁹F, and ³¹P{¹H} NMR spectra.

Perfluoroisopropylation of Acid Chlorides: General Procedure. The copper complex **3b** (50 mg, 0.07 mmol) was loaded into an NMR tube and mixed with DMF. The benzoyl chloride (A mg, 0.05 mmol) was then added to the solution. The reaction was left to sit at room temperature for 24 h. The reaction mixture changed from deep orange-red to light orange with a significant amount of orange precipitate being formed. See Figures S25–S36 for ¹⁹F NMR spectra.

PhC(O)(hfp) (4a). ¹⁹F NMR (282 MHz, DMF): δ -73.95 (d, ³J_{FF} = 7 Hz, CF₃ⁱPr^F), -179.17 (m, ³J_{FF} = 7 Hz, CF^FPr^F). GC-MS (retention time 3.91 min): expected, 274.1; found, 274.1.

3,4,5-(OMe)₃-PhC(O)(hfp) (4b). ¹⁹F NMR (282 MHz, DMF): δ -73.93 (d, ³J_{FF} = 7 Hz, CF₃ⁱPr^F), -177.79 (m, ³J_{FF} = 7 Hz, CF^FPr^F). GC-MS (retention time 7.11 min): expected, 364.1 (100%); found, 364.1 (100%).

p-Me-PhC(O)(hfp) (4c). ¹⁹F NMR (282 MHz, DMF): δ -74.50 (d, ³J_{FF} = 7 Hz, CF₃ⁱPr^F), -179.19 (m, ³J_{FF} = 7 Hz, CF^FPr^F). GC-MS (retention time 4.63 min): expected, 288.1; found, 288.1.

o-Me-PhC(O)(hfp) (4d). ¹⁹F NMR (282 MHz, DMF): δ -74.19 (d, ³J_{FF} = 7 Hz, CF₃ⁱPr^F), -177.46 (m, ³J_{FF} = 7 Hz, CF^FPr^F). GC-MS: (retention time: 4.34 min): expected, 288.1; found, 288.1.

m-Br-Ph(CO)(hfp) (4e). ¹⁹F NMR (282 MHz, DMF): δ -74.50 (d, ³J_{FF} = 7 Hz, CF₃ⁱPr^F), -179.85 (m, ³J_{FF} = 7 Hz, CF^FPr^F). GC-MS (retention time 5.16 min): expected, 351.9 (100%), 353.9 (97.3%); found, 351.9 (100%), 353.9 (93%).

p-F-PhC(O)(hfp) (4f). ¹⁹F NMR (282 MHz, DMF): δ -73.99 (d, ³J_{FF} = 7 Hz, CF₃ⁱPr^F), -101.26 (m, F–Ar), -178.43 (m, ³J_{FF} = 7 Hz, CF^FPr^F). GC-MS (retention time 3.75 min): expected, 292.0 (100%). Found: 291.9 (100%).

p-Br-Ph(CO)(hfp) (4g). ¹⁹F NMR (282 MHz, DMF): δ -73.97 (d, ³J_{FF} = 8 Hz, CF₃ⁱPr^F), -178.90 (d“multiplet”, ³J_{FF} = 8 Hz, CF^FPr^F). GC-MS (retention time 5.22 min): expected, 351.9 (100%), 353.9 (97.3%); found, 352.1 (100%), 354.0 (90%).

p-CN-PhC(O)(hfp) (4i). ¹⁹F NMR (282 MHz, DMF): δ -73.9 (d, ³J_{FF} = 7 Hz, CF₃ⁱPr^F), -179.45 (d“multiplet”, ³J_{FF} = 7 Hz, CF^FPr^F). GC-MS (retention time 5.30 min): expected, 299.0 (100%); found, 299.1 (100%).

p-NO₂-PhC(O)(hfp) (4j). ¹⁹F NMR (282 MHz, DMF): δ -73.87 (d, ³J_{FF} = 7 Hz, CF₃ⁱPr^F), -179.30 (m, ³J_{FF} = 7 Hz, CF^FPr^F). GC-MS: N/A.

o-NO₂-PhC(O)(*hfp*) (**4k**). ¹⁹F NMR (282 MHz, DMF): δ -73.90 (d, ³J_{FF} = 7 Hz, CF₃iPrF), -179.45 (m, ³J_{FF} = 7 Hz, CFⁱPr^F). GC-MS: N/A.

2-Naph(CO)iPrF (**4l**). ¹⁹F NMR (282 MHz, DMF): δ -74.21 (d, ³J_{FF} = 7 Hz, CF₃iPrF), -176.83 (m, ³J_{FF} = 7 Hz, CFⁱPr^F). GC-MS (retention time 6.70 min): expected, 324.0 (100%); found, 324.1 (100%).

2-Tp(CO)iPrF (**4n**). ¹⁹F NMR (282 MHz, DMF): δ -74.32 (d, ³J_{FF} = 7 Hz, CF₃iPrF), -179.83 (m, ³J_{FF} = 7 Hz, CFⁱPr^F). GC-MS (retention time 4.20 min): expected, 280.1 (100%); found, 280.0 (100%).

Synthesis of *p*-F-PhCH₂(*hfp*) (**5a**). ¹⁹F NMR (282 MHz, DMF): δ -75.86 (d, ³J_{FF} = 7 Hz, CF₃iPrF), -115.91 (m, F-Ar), -182.76 (t sept, ³J_{FH} = 24 Hz, ³J_{FF} = 7 Hz, CFⁱPr^F). GC-MS (retention time 3.82 min) expected, 278.0 (100%); found, 278.1 (100%).³⁶ See Figure S36 for ¹⁹F NMR spectra.

Synthesis of *p*-F-PhCH(OH)(*hfp*) (**5b**). ¹⁹F NMR (376.5 MHz, C₆D₆): -70.40 ("quint", ³J_{FF} = ⁴J_{FF} = 9 Hz, CF₃iPrF), -73.23 ("quint", ³J_{FF} = ⁴J_{FF} = 9 Hz, CF₃iPrF), -111.51 (m, F-Ar), -179.55 (d sept, ³J_{FH} = 12 Hz, ³J_{FF} = 9 Hz, CFⁱPr^F). GC-MS (retention time 5.01 min) expected, 294.0 (100%); found, 294.0 (100%).³⁷ See Figures S37 and S38 for ¹⁹F NMR spectra.

Computational Methods. The geometries were optimized at the density functional theory (DFT)³⁸ level with the hybrid B3LYP^{39,40} with the DFT-optimized DZVP2 basis set⁴¹ for H, N, C, F, and P atoms and aug-cc-pVDZ-PP^{42,43} basis sets for M = Ag, Ni, Cu using the Gaussian09 program system.⁴⁴ Vibrational frequencies were calculated to show that the structures were minima. The B3LYP/DZVP2/aug-cc-pVDZ-PP(M) geometries were used to predict the NMR chemical shifts for F (¹⁹F NMR) and P (³¹P NMR) in C₆H₆ using the ADF program system^{45,46} with the BLYP⁴⁷ functional and the TZ2P basis set in ADF.⁴⁸ Scalar relativistic effects were included at the two-component zero-order regular approximation (ZORA) level for the NMR calculations.^{49–51} The ¹⁹F NMR and ³¹P NMR chemical shifts are reported relative to their specific standards CFCl₃ and H₃PO₄ calculated at the same level.

Using the gas-phase geometries, the solvation free energies in DMF at 298 K were calculated using the self-consistent reaction field (SCRF) approach⁵² with the COSMO parameters^{53,54} as implemented in Gaussian 09⁴⁴ at the same B3LYP/DZVP2 level of theory using the COSMO radii. The Gibbs free energy in DMF solution, ΔG_{DMF}, was calculated from eq 1.

$$\Delta G_{\text{DMF}} = \Delta G_{\text{gas}} + \Delta G_{\text{SOLV}} \quad (1)$$

where ΔG_{gas} is the gas phase free energy and ΔG_{solv} is the solvation free energy in DMF. A dielectric constant of 37.22 corresponding to that of bulk DMF was used in the COSMO calculations.

The Natural Population Analysis based on the Natural Bond Orbitals (NBOs)^{55,56} using NBO6^{57,58} with wave functions are calculated at the B3LYP/DZVP2/aug-cc-pVDZ-PP(M) density functional theory level using Gaussian09.

The calculations were performed on a Xeon-based Dell Linux cluster at the University of Alabama, and a local AMD Opteron-based and Intel Xeon-based Linux cluster from Penguin Computing.

■ ASSOCIATED CONTENT

● Supporting Information

This material is available free of charge via the Internet at <http://pubs.acs.org>. The Supporting Information is available free of charge on the ACS Publications website at DOI: 10.1021/acs.organomet.7b00837.

Additional crystallographic information, DFT studies, and ¹H, ¹⁹F, ¹³C{¹H} and ³¹P{¹H} NMR spectra. (PDF) optimized Cartesian coordinates in Å (PDF)

Accession Codes

CCDC 1586727–1586731 contain the supplementary crystallographic data for this paper. These data can be obtained free of

charge via www.ccdc.cam.ac.uk/data_request/cif, or by emailing data_request@ccdc.cam.ac.uk, or by contacting The Cambridge Crystallographic Data Centre, 12 Union Road, Cambridge CB2 1EZ, UK; fax: +44 1223 336033.

■ AUTHOR INFORMATION

Corresponding Author

*E-mail for R.T.B.: rbaker@uottawa.ca.

ORCID

David A. Dixon: 0000-0002-9492-0056

R. Tom Baker: 0000-0002-1133-7149

Notes

The authors declare no competing financial interest.

■ ACKNOWLEDGMENTS

We thank the NSERC and the Canada Research Chairs program for generous financial support and the University of Ottawa, Canada Foundation for Innovation and Ontario Ministry of Economic Development and Innovation for essential infrastructure. NOA gratefully acknowledges support from the province of Ontario, NSERC and the University of Ottawa (OGS and CGS-M/D). The computational work at UA was supported by the Chemical Sciences, Geosciences and Biosciences Division, Office of Basic Energy Sciences, U.S. Department of Energy (DOE) under the DOE BES Catalysis Center Program by a subcontract from Pacific Northwest National Laboratory (KC0301050-47319). DAD also thanks the Robert Ramsay Chair Fund of The University of Alabama for support.

■ REFERENCES

- (1) Banks, R. E.; Smart, B. E.; Tatlow, J. C. *Organofluorine Chemistry: Principles and Commercial Applications*; Plenum: New York, 1994.
- (2) Chambers, R. D. *Fluorine Chemistry at the Millennium*; Elsevier: Amsterdam, 2000.
- (3) Gouverneur, V.; Müller, K. *Fluorine in Pharmaceutical and Medicinal Chemistry*; Imperial College Press: London, 2012.
- (4) Purser, S.; Moore, P. R.; Swallow, S.; Gouverneur, V. *Chem. Soc. Rev.* **2008**, *37*, 320–330.
- (5) Wang, J.; Sánchez-Roselló, M.; Aceña, J. L.; del Pozo, C.; Sorochinsky, A. E.; Fustero, S.; Soloshonok, V. A.; Liu, H. *Chem. Rev.* **2014**, *114*, 2432–2506.
- (6) (a) Charpentier, J.; Früh, N.; Togni, A. *Chem. Rev.* **2015**, *115*, 650–682. (b) Yang, X.; Wu, T.; Phipps, J.; Toste, F. D. *Chem. Rev.* **2015**, *115*, 826–870. (c) Alonso, C.; Martínez de Marigorta, E.; Rubiales, G.; Palacios, F. *Chem. Rev.* **2015**, *115*, 1847–1935. (d) Gao, P.; Song, S.-R.; Liu, X.-Y.; Liang, Y.-M. *Chem. - Eur. J.* **2015**, *21*, 7648–7661. (e) Kyasa, S. *Synlett* **2015**, *26*, 1911–1912. (f) Wang, S.-M.; Han, J.-B.; Zhang, C.-P.; Qin, H.-L.; Xia, J.-C. *Tetrahedron* **2015**, *71*, 7949–7976.
- (7) (a) Hu, J.; Zhang, W.; Wang, F. *Chem. Commun.* **2009**, 7465–7478. (b) Lu, Y.; Liu, C.; Chen, Y.-C. *Curr. Org. Chem.* **2015**, *19*, 1638–1650. (c) Chen, B.; Vicio, D.. Transition-Metal-Catalyzed Difluoromethylation, Difluoromethylenation, and Polydifluoromethylenation Reactions. In *Organometallic Fluorine Chemistry*; Braun, T., Hughes, R. P., Eds.; Springer US: New York, 2014; Topics in Organometallic Chemistry *S2*, pp 113–141. (d) Serizawa, H.; Ishii, K.; Aikawa, K.; Mikami, K. *Org. Lett.* **2016**, *18*, 3686–3689.
- (8) (a) Huang, Y.; Ajitha, M. J.; Huang, K.-W.; Zhang, Z.; Weng, Z. *Dalton Trans.* **2016**, *45*, 8468–8474. (b) Sugiishi, T.; Amii, H.; Aikawa, K.; Mikami, K. *Beilstein J. Org. Chem.* **2015**, *11*, 2661–2670. (c) Li, L.; Ni, C.; Xie, Q.; Hu, M.; Wang, F.; Hu, J. *Angew. Chem., Int. Ed.* **2017**, *56*, 9971–9975.
- (9) (a) Landelle, G.; Panossian, A.; Leroux, F. R. *Curr. Top. Med. Chem.* **2014**, *14*, 941–951. (b) Lee, K.; Lee, J.; Ngai, M.-Y. *Synlett*

- 2016, 27, 313–319. (c) Basset, T.; Jubault, P.; Pannecoucke, X.; Poisson, T. *Org. Chem. Front.* **2016**, 3, 1004–1010.
- (10) (a) Landelle, G.; Panossian, A.; Pazenok, S.; Vors, J.-P.; Leroux, F. R. *Beilstein J. Org. Chem.* **2013**, 9, 2476–2536. (b) Barata-Vallejo, S.; Bonesi, S.; Postigo, A. *Org. Biomol. Chem.* **2016**, 14, 7150–7182.
- (11) (a) Tohnishi, M.; Nakao, H.; Kohno, E.; Nishida, T.; Furuya, T.; Shimizu, T.; Seo, A.; Sakata, K.; Fujioka, S.; Kanno, H. EP 919542, 1999. (b) Tohnishi, M.; Nakao, H.; Kohno, E.; Nishida, T.; Furuya, T.; Shimizu, T.; Seo, A.; Sakata, K.; Fujioka, S.; Kanno, H. EP 1006107, 2000. (c) Kimura, M.; Morimoto, M.; Uehara, M.; Watanabe, M.; Yoshida, M. EP 1097932A1, 2001. (d) Zhang, J.; Tang, X.; Ishaaya, I.; Cao, S.; Wu, J.; Yu, J.; Li, H.; Quain, X. *J. Agric. Food Chem.* **2010**, 58, 2736–2740. Zhou, S.; Meng, X.; Jin, R.; Ma, Y.; Xie, Y.; Zhao, Y.; Song, H.; Xiong, L.; Li, Z. *Mol. Diversity* **2017**, 21, 915.
- (12) Prakash, G. K. S.; Hu, J.; Olah, G. A. *J. Org. Chem.* **2003**, 68, 4457–4463.
- (13) Lishchynskyi, A.; Grushin, V. V. *J. Am. Chem. Soc.* **2013**, 135, 12584–12587.
- (14) Xu, L.; Vacic, D. A. *J. Am. Chem. Soc.* **2016**, 138, 2536–2539.
- (15) Morimoto, H.; Tsubogo, T.; Litvinas, N. D.; Hartwig, J. F. *Angew. Chem., Int. Ed.* **2011**, 50, 3793–3798.
- (16) (a) Ishikawa, N.; Shin-ya, S. *Bull. Chem. Soc. Jpn.* **1975**, 48, 1339–1340. (b) Takechi, N.; Ait-Mohand, S.; Médebielle, M.; Dolbier, W. R., Jr. *Tetrahedron Lett.* **2002**, 43, 4317–4319.
- (17) (a) Naumann, D.; Finke, M.; Lange, H.; Dukat, W.; Tyrre, W. *J. Fluorine Chem.* **1992**, 56, 215–237. (b) Chambers, R. D.; Musgrave, W. K. R.; Savory, J. *J. Chem. Soc.* **1962**, 0, 1993–1991. (c) Nair, H. K.; Burton, D. J. *J. Fluorine Chem.* **1992**, 56, 341–351. (d) Ishikawa, N.; Ochiai, M. *Nippon Kagaku Kaishi* **1973**, 1973, 2351–2356. (e) McLoughlin, V. C. R.; Thrower, J. *Tetrahedron* **1969**, 25, 5921–5940. (f) Burch, R. R.; Calabrese, J. C. *J. Am. Chem. Soc.* **1986**, 108, 5359–5360. (g) Naumann, D.; Wessel, W.; Hahn, J.; Tyrre, W. *J. Organomet. Chem.* **1997**, 547, 79–88. (h) Bubot, G.; Mansuy, D.; Lecolier, S.; Normant, J. F. *J. Organomet. Chem.* **1972**, 42, C105–C106. (i) Sekiya, A.; Ishikawa, N. *Chem. Lett.* **1977**, 6, 81–84.
- (18) (a) Toscano, P. J.; Brand, H.; Geremia, S.; Randaccio, L.; Zangrando, E. *Organometallics* **1991**, 10, 713–720. (b) Jiang, D.-F.; Liu, C.; Guo, Y.; Xiao, J.-C.; Chen, Q.-Y. *Eur. J. Org. Chem.* **2014**, 2014, 6303–6309.
- (19) (a) Miller, W. T.; Burnard, R. J. *J. Am. Chem. Soc.* **1968**, 90, 7367–7368. (b) Dyatkin, B. L.; Martynov, B. I.; Martynova, L. G.; Kizim, N. G.; Sterlin, S. R.; Stumbrevichute, Z. A.; Fedorov, L. A. *J. Organomet. Chem.* **1973**, 57, 423–433.
- (20) (a) Simon, C. M.; Kaminsky, W. *Polym. Degrad. Stab.* **1998**, 62, 1–7. (b) Van der Walt, I. J.; Grunenburg, A. T.; Nel, J. T.; Maluleke, G. G.; Bruinsma, S. L. *J. Appl. Polym. Sci.* **2008**, 109, 264–271.
- (21) (a) Li, Y.; Wang, X.; Guo, Y.; Zhu, Z.; Wu, Y.; Gong, Y. *Chem. Commun.* **2016**, 52, 796–799. (b) Wang, X.; Li, Y.; Guo, Y.; Zhu, Z.; Wu, Y.; Cao, W. *Org. Chem. Front.* **2016**, 3, 304–308. (c) Liu, X.-H.; Leng, J.; Jia, S.-J.; Hao, J.-H.; Zhang, F.; Qin, H.-L.; Zhang, C. P. *J. Fluorine Chem.* **2016**, 189, 59–67.
- (22) Zeng, Y.; Zhang, L.; Zhao, Y.; Ni, C.; Zhao, J.; Hu, J. *J. Am. Chem. Soc.* **2013**, 135, 2955–2958.
- (23) Example of successful transmetalation with silver perfluoroalkyl to nickel: Zhang, C.-P.; Wang, H.; Klein, A.; Biewer, C.; Stirnat, K.; Yamaguchi, Y.; Xu, L.; Gomez-Benitez, V.; Vacic, D. A. *J. Am. Chem. Soc.* **2013**, 135, 8141–8144.
- (24) Examples of M–RF compounds with elongated C_α–F bonds: (a) Hughes, R. P. *J. Fluorine Chem.* **2010**, 131, 1059–1070. (b) Goodman, J.; Grushin, V. V.; Larichev, R. B.; Macgregor, S. A.; Marshall, W. J.; Roe, D. C. *J. Am. Chem. Soc.* **2009**, 131, 4236–4238. (c) Garratt, S. A.; Hughes, R. P.; Kovacic, I.; Ward, A. J.; Willemsen, S.; Zhang, D. *J. Am. Chem. Soc.* **2005**, 127, 15585–15594. (d) Torrens, H. *Coord. Chem. Rev.* **2005**, 249, 1957–1985. (e) Huang, D.; Koren, P. R.; Folting, K.; Davidson, E. R.; Caulton, K. G. *J. Am. Chem. Soc.* **2000**, 122, 8916–8931. (f) Richmond, T. G.; Shriver, D. F. *Organometallics* **1984**, 3, 314–319. (g) Richmond, T. G.; Shriver, D. F. *Organometallics* **1983**, 2, 1061–1062. (h) Andrella, N. O.; Sicard, A. J.; Gorelsky, S. I.; Korobkov, I.; Baker, R. T. *Chem. Sci.* **2015**, 6, 6392–6397. (i) Harrison, D. J.; Daniels, A. L.; Korobkov, I.; Baker, R. T. *Organometallics* **2015**, 34, 4598–4604.
- (25) (a) Gulliver, D. J.; Levason, W.; Webster, M. *Inorg. Chim. Acta* **1981**, 52, 153–159. (b) Chaudhuri, M. K.; Dhar, S. S.; Viayashree, N. *Transition Met. Chem.* **2000**, 25, 559–561.
- (26) Larsson, J. M.; Pathipati, S. R.; Szabó, K. J. *J. Org. Chem.* **2013**, 78, 7330–7336.
- (27) Tomashenko, O. A.; Escudero-Adán, E. C.; Belmonte, M. M.; Grushin, V. V. *Angew. Chem., Int. Ed.* **2011**, 50, 7655–7659.
- (28) Panferova, L. I.; Miloserdov, F. M.; Lishchynskyi, A.; Belmonte, M. M.; Benet-Buchholz, J.; Grushin, V. V. *Angew. Chem., Int. Ed.* **2015**, 54, 5218–5222.
- (29) Kikushima, K.; Sakaguchi, H.; Saijo, H.; Ohashi, M.; Ogoshi, S. *Chem. Lett.* **2015**, 44, 1019–1021. More recently, oxycupration: Ohashi, M.; Adachi, T.; Ishida, N.; Kikushima, K.; Ogoshi, S. *Angew. Chem., Int. Ed.* **2017**, 56, 11911–11915.
- (30) Lv, H.; Cai, Y.-B.; Zhang, J.-L. *Angew. Chem., Int. Ed.* **2013**, 52, 3203–3207.
- (31) It should be noted that the scope of both referenced reactions was quite limited.
- (32) The vacuum transfer procedure was done for **4f** and **4n**.
- (33) Note that **3b** undergoes homolysis at room temperature only in the presence of an electrophile.
- (34) (a) Zhu, F.; Yang, G.; Zhou, S.; Wu, X.-F. *RSC Adv.* **2016**, 6, 57070–57074. (b) Braun, T.; Parsons, S.; Perutz, R. N.; Voith, M. *Organometallics* **1999**, 18, 1710–1716.
- (35) Curtiss, L. A.; Redfern, P. C.; Raghavachari, K.; Rassolov, V.; Pople, J. A. *J. Chem. Phys.* **1999**, 110, 4703–4709.
- (36) Characterization data match those of some reported benzyl-hfip and analogous alkyl-hfip compounds: (a) Dneprovskii, A. S.; Kasatochkin, A. N.; Kondakov, D. Y. *Russ. J. Org. Chem.* **1989**, 25, 1984–1991. (b) Ignatowska, J.; Wojciech, D. *J. Fluorine Chem.* **2007**, 128, 997–1006.
- (37) Characterization data match those of some reported arylcarbinol-hfip compounds: (a) O’Reilly, N. J.; Maruta, M.; Ishikawa, N. *Chem. Lett.* **1984**, 13, 517–520. (b) Kitazume, T.; Ishikawa, N. *J. Am. Chem. Soc.* **1985**, 107, 5186–5191. (c) Kitazume, T.; Ishikawa, N. *Chem. Lett.* **1981**, 10, 1337–1338.
- (38) Parr, R. G.; Yang, W. *Density-Functional Theory of Atoms and Molecules*; Oxford University Press: New York, 1989.
- (39) Becke, A. D. *J. Chem. Phys.* **1993**, 98, S648–S652.
- (40) Lee, C.; Yang, W.; Parr, R. G. *Phys. Rev. B: Condens. Matter Mater. Phys.* **1988**, 37, 785–789.
- (41) Godbout, N.; Salahub, D. R.; Andzelm, J.; Wimmer, E. *Can. J. Chem.* **1992**, 70, S60–S71.
- (42) Peterson, K. A.; Puzzarini, C. *Theor. Chem. Acc.* **2005**, 114, 283–296.
- (43) Peterson, K. A.; Figgen, D.; Dolg, M.; Stoll, H. *J. Chem. Phys.* **2007**, 126, 124101.
- (44) Frisch, M. J.; Trucks, G. W.; Schlegel, H. B.; Scuseria, G. E.; Robb, M. A.; Cheeseman, J. R.; Scalmani, G.; Barone, V.; Mennucci, B.; Petersson, G. A., et al. *Gaussian 09, Revision A.2*; Gaussian, Inc., Wallingford, CT, 2009.
- (45) te Velde, G.; Bickelhaupt, F. M.; van Gisbergen, S. J. A.; Fonseca Guerra, C.; Baerends, E. J.; Snijders, J. G.; Ziegler, T. *J. Comput. Chem.* **2001**, 22, 931–967.
- (46) *ADF 2017, ADF Users Guide*; SCM, Theoretical Chemistry, Vrije Universiteit: Amsterdam; <http://www.scm.com>, Accessed 6-15-2017.
- (47) Becke, A. D. *Phys. Rev. A: At., Mol., Opt. Phys.* **1988**, 38, 3098–3100.
- (48) *ADF 2008.01, ADF Users Guide*; SCM, Theoretical Chemistry, Vrije Universiteit: Amsterdam, 2008; <http://www.scm.com>.
- (49) Wolff, S. K.; Ziegler, T.; van Lenthe, E.; Baerends, E. J. *J. Chem. Phys.* **1999**, 110, 7689–7698.
- (50) van Lenthe, E.; Baerends, E. J.; Snijders, J. G. *J. Chem. Phys.* **1993**, 99, 4597–4610.

(51) Autschbach, J.; Ziegler, T. In *Calculation of NMR and EPR Parameters: Theory and Application*, Kaupp, M., Buhl, M., Malkin, V. G., Eds.; Wiley-VCH: Weinheim, Germany, 2004; pp 249–264.

(52) Tomasi, J.; Mennucci, B.; Cammi, R. *Chem. Rev.* **2005**, *105*, 2999–3093.

(53) Klamt, A. *Quantum Chemistry to Fluid Phase Thermodynamics and Drug Design*; Elsevier: Amsterdam, 2005.

(54) Klamt, A.; Schüürmann, G. *J. Chem. Soc., Perkin Trans. 2* **1993**, *2*, 799–805.

(55) Reed, A. E.; Curtiss, L. A.; Weinhold, F. *Chem. Rev.* **1988**, *88*, 899–926.

(56) Weinhold, F.; Landis, C. R. *Valency and Bonding: A Natural Bond Orbital Donor-Acceptor Perspective*; University Press: Cambridge, U.K., 2005.

(57) Glendening, E. D.; Badenhop, J. K.; Reed, A. E.; Carpenter, J. E.; Bohmann, J. A.; Morales, C. M.; Landis, C. R.; Weinhold, F. *Natural Bond Order 6.0*; Theoretical Chemistry Institute, University of Wisconsin, Madison, WI, 2013; <http://nbo6.chem.wisc.edu/>, accessed 12–01-2013.

(58) Glendening, E. D.; Landis, C. R.; Weinhold, F. *J. Comput. Chem.* **2013**, *34*, 1429–1437.

(59) Prepared by a modification of procedure for (2-methylpyridine)₂NiBr₂: Vallarino, L. M.; Hill, W. E.; Quagliano, J. V. *Inorg. Chem.* **1965**, *4*, 1598–1604.